EUROPEAN ORGANIZATION FOR NUCLEAR RESEARCH

Proposal to the ISOLDE and Neutron Time-of-Flight Committee

Onset of collective structures in proton-rich Pb isotopes investigated via fast-timing methods.

September 26, 2023

J. Benito[1], A. Illana[2], A.N. Andreyev[3], P. Aguilera[1], A. Algora[4], O. Alonso-Sañudo[2], G. de Angelis[5], M. Balogh[5], M.J.G. Borge[6], A.D. Briscoe[7], J.A. Briz[2], D. Brugnara[5], S. Carollo[1], T.E. Cocolios[8], J.G. Cubiss[3], R. Escudeiro[1], A. Ertoprak[5], J.L. Herraiz[2], L.P. Gaffney[7], F. Galtarossa[5], A. Goasduff[5], B. Gongora[5], A. Gottardo[5], L.M. Fraile[2], J. Jolie[9], A. Korgul[10], S.M. Lenzi[1], R. Liča[11], M. Llanos[2], N. Marginean[11], R. Marginean[11], R. Menegazzo[1] , D. Mengoni[1], C. Mihai[11], E. Nácher[4], D.R. Napoli[5], A. Negret[11], C.R. Nita[11], V. Nouvilas[2], J. Ojala[7], B. Olaizola[6], C. Page[3], R.D. Page[7], J. Pakarinen[12,13], P. Papadakis[14], S. Pascu[11], A. Perea[6], J. Pellumaj[5], R.M. Pérez-Vidal[5], S. Pigliapoco[1], A.M. Plaza[7,12], F. Recchia[1], K. Rezynkina[1], J. Romero[7], F. Rotaru[11], B. Rubio[4], C. Sotty[11], M. Stryjczyk[12,13], O. Tengblad[6], J.J. Valiente-Dobón[5], P. Van Duppen[8], N. Warr[9], H. de Witte[8], Z. Yue[3], L. Zago[5], and the IDS Collaboration

[1] *Dipartimento di Fisica and INFN, Sezione di Padova, Padova, Italy.*
[2] *Grupo de Física Nuclear & IPARCOS, Universidad Complutense de Madrid, Madrid, Spain.*
[3] *School of Physics, Engineering and Technology, University of York, York, YO10 5DD, UK.*
[4] *Instituto de Física Corpuscular, CSIC and Universidad de Valencia, Paterna, Spain.*
[5] *INFN, Laboratori Nazionali di Legnaro, Legnaro, Italy.*
[6] *Instituto de Estructura de la Materia, CSIC, Madrid, Spain.*
[7] *Oliver Lodge Laboratory, University of Liverpool, Liverpool, L69 7ZE, UK.*
[8] *KU Leuven, Instituut voor Kern- en Stralingsfysica, 3001 Leuven, Belgium.*
[9] *Institut für Kernphysik, Universität zu Köln, Köln, Germany.*
[10] *Faculty of Physics, University of Warsaw, Warsaw, Poland.*
[11] *"Horia Hulubei" National Institute of Physics and Nuclear Engineering, Bucharest, Romania.*
[12] *Accelerator Laboratory, Department of Physics, University of Jyväskylä, Jyväskylä, Finland.*
[13] *Helsinki Institute of Physics, Helsinki, Finland.*
[14] *STFC Daresbury Laboratory, Daresbury, Warrington, WA4 4AD, UK.*

CERN-INTC-2023-073 / INTC-P-680
26/09/2023

Spokesperson: J. Benito [jaime.benito@pd.infn.it] and A. Illana [andres.illana@ucm.es]
Contact person: H. Heylen (hanne.heylen@cern.ch)

Abstract: The Z=82 neutron-deficient Pb region is very well-known due to the occurrence of shape-coexistence phenomena. This feature has motivated a large number

of studies. However, the information about low-lying level lifetimes below the ns range is very scarce. In order to establish a complete picture of shape coexistence in this region, information on transition probabilities from nuclear states assigned to different shapes is essential. We propose to perform a systematic study of the Pb isotopes in the range $^{191-198}$Pb populated in the β-decay of bismuth isotopes. The well-established fast-timing technique will be employed to measure the lifetimes of the excited levels. The lifetime measurements in even-even lead will provide detailed information about the development of oblate $\pi(2p-2h)$ configurations and their mixing with spherical configurations. Moreover, we propose to perform an investigation of the mixing between configurations in the low-lying states of the neutron-deficient $^{191-197}$Pb isotopes. Transition rates between quasiparticle configurations built on spherical and intruder configurations will provide key information on the collectivity and the development of shape coexistence.

Requested shifts: 17 shifts, (split into 1 runs over 1 years)
Installation: ISOLDE Decay station

1 Physics case

The interplay between single-particle motion, collectivity and pairing in the atomic nucleus is seen as a rich tapestry of coexisting shapes and exotic excitations, often associated with so-called intruder states. Spherical shell-model excitations are dominant in the region near the doubly closed-shell nuclei, such as ^{208}Pb. However, collective modes of start to be competitive when approaching the vicinity of the neutron mid-shell region [1, 2, 3, 4]. In the neutron-deficient lead isotopes, the deformed structures appear in the form of oblate and prolate bands, whose excitation energy decreases with decreasing neutron number. Microscopically, the appearance of these bands is associated with the occurrence of oblate $\pi(2p-2h)$ and prolate $\pi(4p-4h)$ excitations across the closed $Z = 82$ proton gshell [5], see Fig 1.a). Hence, different shapes coexist within one nucleus at low energy, the so-called shape coexistence phenomenon. This has been a hot topic in nuclear physics since it was first established by measuring the change in the nuclear charge radius between ^{187}Hg and ^{185}Hg in the early 1970s [6]. Shape coexistence has been observed and studied along the nuclear chart. In particular, several studies have been published solely focusing on the lead nuclei [7, 8, 9, 10, 11, 12].

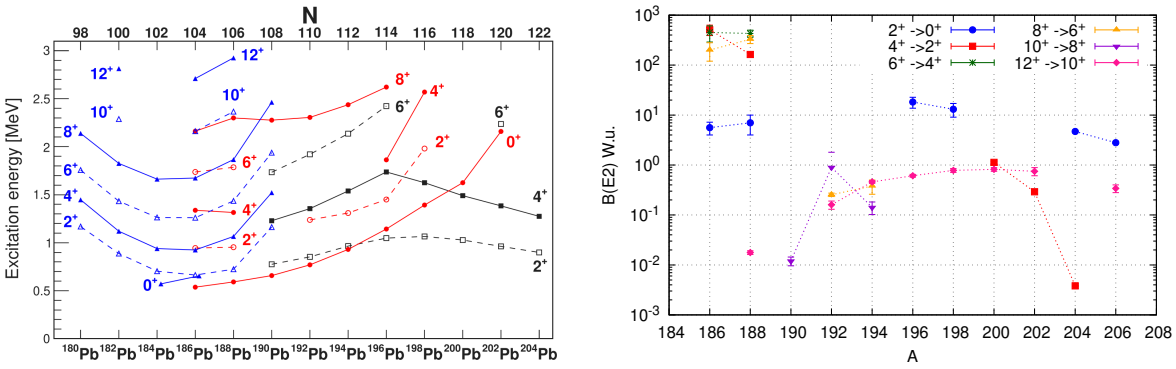

Figure 1: (Left or a) Energy systematic of positive-parity states in the neutron-deficient even-even lead isotopes, showing presumed spherical states (black squares), deformed $\pi(2p-2h)$ configuration (red circles), and deformed $\pi(4p-4h)$ (blue triangles). Figure taken from [4]. (Right or b) Systematic of B(E2) transitions in even-even Pb isotopes. Data taken from ENDSF [13].

Recent theoretical efforts have been made to link the phenomenon of shape coexistence to changes in the single-particle orbits (called "shell evolution") due to nuclear forces. Changes in shell structure across isotopic chains have long been attributed to the effects of the tensor interaction and how spherical single-particle energies are shifted as protons or neutrons occupy certain orbits [14]. In the lead region, neutron particle-hole excitations from the $1h_{9/2}$ orbit to the $1i_{13/2}$ orbit cause a reduction in the proton spin-orbit splitting, implying a reduction of the $1h_{11/2}$ - $1h_{9/2}$ gap [15]. This has been coined "type II shell evolution". Due to type II shell evolution, the single-particle energies can be re-arranged with a reduced spin-orbit interaction [16, 17]. This implies weaker resistance against deformation, and a strongly deformed local minimum may

occur. Key to help the understanding of this phenomenon is accurate knowledge of the transition probabilities between the low-lying states.

Electromagnetic transition strengths can be extracted from the lifetimes of the excited levels and γ branching ratios. Thus, completing the information about half-lives of excited states in this region is highly valuable information to characterize the onset of deformation. The available lifetime measurements are scarce in this region, since only long-lived ns$-\mu s$ states have been measured by electronic delayed coincidence methods γ(t) with HPGe detectors. The presence of these isomers hampers the measurement of the short-lived states located below. Experiments employing the Recoil Doppler-Shift method in fusion-evaporation reactions are very challenging due to the predominant feeding of these levels. In addition, Coulomb excitation experiments employing radioactive ion beams have been attempted [18], however, only $B(E2; 2^+ \rightarrow 0^+)$ for the ^{196}Pb and ^{198}Pb isotopes have been successfully measured. Alternatively, we propose to measure these lifetimes by employing the ultra-fast $LaBr_3$(Ce) detectors in β-decay experiments, using the fast-timing technique [19, 20].

1.1 Even-even Pb isotopes

Information on lifetimes of excited levels is mostly limited to the $J = 12^+$ seniority level, or to negative parity bands weakly connected with the positive parity low-lying levels. The lifetimes of yrast-bands in ^{186,188}Pb have been measured up to $J = 8$ in fusion-evaporation reactions [21, 10], confirming the nature of the oblate and deformed bands, and measuring their deformation parameters. Nevertheless, this information is missing for more neutron-rich isotopes, see Fig. 1.a). For the isotopes heavier than ^{190}Pb, the prolate deformed bands are expected to go higher in energy, and therefore, the low-lying states should correspond to either spherical or $\pi(2p - 2h)$ configurations. The experimental 2^+_1, 4^+_1 and 6^+_1 states beyond ^{190}Pb have been associated with spherical configurations. Nevertheless, the Interacting Boson Model (IBM) [5], indicates that the 4^+_1 and 6^+_1 states in $^{190-194}$Pb, have a major, even dominant $\pi(2p - 2h)$ character, or at least, they are strongly mixed with the spherical 4^+ and 6^+ states.

The experimentally identified 8^+ states were related to strongly mixed oblate, spherical, and prolate states. In particular, the 8^+_1 state in ^{192,194}Pb is suggested to be associated with deformed two proton configuration, $\pi f_{7/2}h_{9/2}$, with the oblate deformation [22]. Systematic comparison with neighbouring nuclei supports an oblate deformation for the 8^+_1 state [23]. The first 8^+ state was identified as isomeric with $B(E2; 8^+ \rightarrow 6^+)$=0.25(3) W.u. and $B(E2; 8^+ \rightarrow 6^+)$=0.14(4) W.u. for ^{192}Pb and ^{194}Pb, respectively [24, 8]. This indicates a small but growing mixing of oblate deformation in the 6^+ state with decreasing neutron number [22]. However, this contradicts the aforementioned deformed $\pi(2p - 2h)$ nature predicted for the 4^+_1 and 6^+_1 states [5], which rather suggested a strong collective $B(E2; 8^+ \rightarrow 6^+)$. Clarifying the structure of the 4^+_1 and 6^+_1 states will lead us to understand the nature of the 8^+ states.
In summary, we aim to perform a systematic measurement of lifetimes in the $^{192-198}$Pb

isotopes, in order to characterize the development of deformation. The main aim will be to extract the lifetimes of the 4^+ and 6^+ states, for which lifetimes in the range of 10-100 ps can be expected, according to systematics and theoretical predictions [5]. This will be the first fast-timing study performed in these isotopes, which will provide information on the lifetimes of the low-lying states from ns to ∼10 ps. If statistics suffice, lifetimes for higher lying states $J = 10$ can be extracted, providing information on the interplay between deformed and spherical configurations. The use of RILIS in narrow-band mode will make isomeric selection possible and will allow us to disentangle the feeding from the different β-decaying states.

1.2 Odd-even Pb isotopes

The low energy states in the odd-Pb isotopes provide important information about the interplay of single-particle configurations with collective structures. In a naive shell-model interpretation, the low-lying states in the odd-A Pb isotopes can be identified as single neutrons coupled to the spherical g.s. in the even-even nuclei, see Fig. 2. Measuring the $B(M1)$ and $B(E2)$ values will provide important information about how collectivity develops in the g.s. spherical configuration. In particular, we aim to perform the systematic measurement lifetimes for the $5/2^-_1$ states in the 191-197 mass range, in order to obtain complete l-forbidden M1 $\nu 2f_{5/2} \rightarrow 3p_{3/2}$ transition. Above the $(3/2^-)$ g.s. and $(13/2^+)$, a set of intruders $(13/2^+)$ and $(3/2^-)$ states have been identified in $^{189-197}$Pb [25, 26, 27], which are interpreted $\nu 1i_{13/2}$ or $\nu 3p_{3/2}$ neutrons coupled to the deformed 0^+ intruder states. The lifetimes of these levels, which are de-excited by highly converted $E0 + M1 + E2$ transitions, provide important information about the $E0$ matrix element, and thus the $\rho(E0)$. This quantity will provide important information about the mixing between these intruders and spherical configurations. In this experiment, we will aim to extract the lifetimes of these intruder states, whose lifetimes are expected in the range of tens of ps.

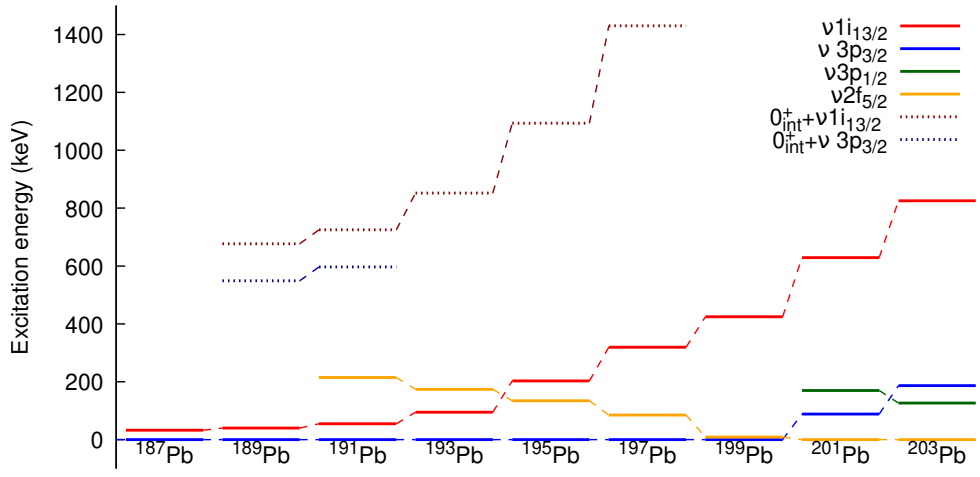

Figure 2: Systematic of the single-particle states in odd-even lead isotopes [13].

Focusing on the lighter ^{191,193}Pb isotopes, the information about their level schemes populated in β-decay is still missing. Only a set of γ-rays, which are not placed in the level scheme, are known [28], and thus the known levels correspond mostly to high-spin levels populated in fusion-evaporation experiments. In the most neutron-deficient nuclei, alpha decay studies proved the presence of intruder states at low energies [28, 25]. Hence, the excellent yields for bismuth isotopes at ISOLDE will allow us to perform a detailed study of their low-lying states, to build their level schemes, and to characterize the interplay between intruder and spherical configuration. The expected statistics will also allow us to extract lifetimes from ns to tens of ps using the fast-timing technique.

2 Experimental details

The neutron-deficient bismuth beams were produced in the past with high yields [29] using UC_X targets and the RILIS system. We propose to use the same type of primary target with a desirable proton beam intensity of 2 μA. The neutron-deficient bismuth beams will be isomerically selected by the ISOLDE-RILIS system [30], and transported to the ISOLDE Decay Station (IDS). The use of RILIS also grants isomeric selectivity, by taking advantage of the difference in the hyperfine splitting of the isomers and ground state. The Bi laser ionization scheme is already available as indicated in the RILIS database [30]. However, a high degree of isobaric contamination coming from the surface-ionized Tl isotopes is expected in the region of interest, which is almost in the same order of magnitude as the production of the isobaric bismuth for the most exotic case, $A = 192$ [29]. Fortunately, the Bi isotopes decay one order of magnitude faster than Tl. Hence, it will be possible to control the influence of the isobaric contaminants by making use of the IDS tape station, where the ions are implanted. Nevertheless, we will also need to collect data using the laser-off mode to address the impact of the isobaric contamination for each case.

The proposed β-decay experiment will use the IDS setup consisting of the tape station equipped with a fast plastic scintillator close to the implantation point having almost 25% efficiency for β detection, coupled to a combination of a minimum of six HPGe clover-type detectors and two $LaBr_3$ (Ce) detectors to register β-delayed γ-rays for the fast-timing measurement. The expected total photopeak efficiency of the Clover detectors will be 6% at 1.0 MeV and 1% at 0.8 MeV for the $LaBr_3$ (Ce) detectors. The present intensity of the Bi beams will allow us to perform γ-γ coincidence studies to define the correct transition sequences and be able to discriminate transitions populated by the possible contaminants. The use of fast $LaBr_3$ (Ce) detectors will give us access to lifetime information in the tens of picoseconds range on the states in the daughter nuclei, and therefore we will also be able to get information on the reduced transition probabilities. The yields expected, the number of counts per shift, and the number of shifts required for each Bi isotope are shown in Table 1. The yields have been estimated, assuming a 70% transmission efficiency to the IDS, and 5% of ionization efficiency of isomer selection. For the isotopes heavier than 193, count rates have been estimated assuming a maximum implantation rate of $5{\cdot}10^4$ pps. This value was deduced from previous fast-timing experiments as an upper limit for maximum rates that the IDS detectors can withstand. The counting rates

have been estimated considering the average expected feeding to the level of interest. Given the strong predominance of EC channel with respect to the total β^+/EC decay intensity, a 30-50% of β^+ intensity was considered, based on the systematics of the region.

Isotope	$T_{1/2}$	Yield [ions/μC]	Ions/s IDS	β-γ_{LaBr}-γ_{LaBr} [Counts/shift]	β-γ_{LaBr}-γ_{Ge} [Counts/shift]	Shifts
^{192g}Bi (3^+)	34 s	$3.6{\cdot}10^4$	$2.5{\cdot}10^3$	$1.6{\cdot}10^3$	$4.5{\cdot}10^2$	1.5
^{192m}Bi (10^-)	39 s	$1.1{\cdot}10^5$	$7.7{\cdot}10^3$	$4.9{\cdot}10^3$	$1.4{\cdot}10^3$	1.5
^{194g}Bi (3^+)	95 s	$1.6{\cdot}10^7$	$5{\cdot}10^4$	$3.5{\cdot}10^4$	$1.0{\cdot}10^4$	0.33
^{194m1}Bi (6^+,7^+)	125 s	$1.6{\cdot}10^7$	$5{\cdot}10^4$	$3.5{\cdot}10^4$	$1.0{\cdot}10^4$	0.33
^{194m2}Bi (10^-)	115 s	$1.6{\cdot}10^7$	$5{\cdot}10^4$	$3.5{\cdot}10^4$	$1.0{\cdot}10^4$	0.33
^{196g}Bi (3^+)	308 s	$2.2{\cdot}10^7$	$5{\cdot}10^4$	$5.3{\cdot}10^3$	$1.5{\cdot}10^3$	0.5
^{196m2}Bi (10^-)	240 s	$2.2{\cdot}10^7$	$5{\cdot}10^4$	$3.9{\cdot}10^3$	$1.1{\cdot}10^3$	0.5
^{198g}Bi (2^+,3^+)	10.3 min	$1.0{\cdot}10^7$	$5{\cdot}10^4$	$3.5{\cdot}10^4$	$1.0{\cdot}10^4$	0.5
^{198m1}Bi (7^+)	1.6 min	$1.0{\cdot}10^7$	$5{\cdot}10^4$	$3.5{\cdot}10^4$	$1.0{\cdot}10^4$	0.5
^{191g}Bi ($9/2^-$)	11.7 s	$3.0{\cdot}10^4$	$2.1{\cdot}10^3$	$1.5{\cdot}10^2$	$7.3{\cdot}10^2$	3
^{193g}Bi ($9/2^-$)	63.6 s	$3.0{\cdot}10^6$	$5{\cdot}10^4$	$6.8{\cdot}10^3$	$3.4{\cdot}10^4$	0.5
^{193m}Bi ($1/2^+$)	3.2 s	$4.0{\cdot}10^4$	$2.8{\cdot}10^3$	$6.3{\cdot}10^1$	$3.2{\cdot}10^2$	1.5
^{195g}Bi ($9/2^-$)	183 s	$1.4{\cdot}10^7$	$5{\cdot}10^4$	$1.0{\cdot}10^3$	$5.2{\cdot}10^3$	0.5
^{195m}Bi ($1/2^+$)	87 s	$1.4{\cdot}10^7$	$5{\cdot}10^4$	$4.7{\cdot}10^3$	$2.4{\cdot}10^4$	0.5
^{197g}Bi ($9/2^-$)	9.33 min	$1.1{\cdot}10^7$	$5{\cdot}10^4$	$1.1{\cdot}10^3$	$5.3{\cdot}10^3$	0.5
^{197m}Bi ($1/2^+$)	5.04 min	$1.1{\cdot}10^7$	$5{\cdot}10^4$	$3.2{\cdot}10^3$	$1.6{\cdot}10^4$	0.5

Table 1: Summary of the yields expected, counts expected for the most relevant transitions applying β-γ_{LaBr}-γ_{LaBr} and β-γ_{LaBr}-γ_{Ge} coincidences, and the shifts estimated for ^{192,198}Pb. For the lighter isotopes, only the β-decay branch has been taken into account.

Summary of requested shifts: We request 17 shifts in total for the $^{191-198}$Bi isotopes. In addition, we will need 1 shift to measure yields and release curves using the IDS/ISOLDE tape station, 1 shift for laser optimization (narrow-band mode), and 2 shifts for fast-timing calibrations (^{138}Cs, ^{140}Ba, ^{88}Rb and ^{24}Na).

References

[1] K. Heyde and J. L. Wood. Shape coexistence in atomic nuclei. *Rev. Mod. Phys.*, 83:1467–1521, Nov 2011.

[2] R. Julin et al. In-beam spectroscopic studies of shape coexistence and collectivity in the neutron-deficient Z $\approx$ 82 nuclei. *Journal of Physics G: Nuclear and Particle Physics*, 43(2):024004ev, feb 2016.

[3] J. Wood and K. Heyde. A focus on shape coexistence in nuclei. *J. of Phys. G*, 43(2):020402, feb 2016.

[4] P. Garrett et al. An experimental view on shape coexistence in nuclei. *Progress in Particle and Nuclear Physics*, 124:103931, may 2022.

[5] V. Hellemans et al. Configuration mixing in the neutron-deficient $^{186-196}$Pb isotopes. *Phys. Rev. C*, 77:064324, Jun 2008.

[6] J. Bonn et al. Sudden change in the nuclear charge distribution of very light mercury isotopes. *Phys. Lett. B*, 38(5):308–311, 1972.

[7] P. Van Duppen et al. Observation of low-lying $J^\pi = 0^+$ states in the single-closed-shell nuclei $^{192-198}$Pb. *Phys. Rev. Lett.*, 52:1974–1977, May 1984.

[8] P. Van Duppen et al. β^+/electron-capture decay of ^{192},194,196,198,200bi: Experimental evidence for low lying 0^+ states. *Phys. Rev. C*, 35:1861–1877, May 1987.

[9] A. Andreyev et al. A triplet of differently shaped spin-zero states in the atomic nucleus ^{186}Pb. *Nature*, 405(6785):430–433, may 2000.

[10] T. Grahn et al. Collectivity and Configuration Mixing in ^{186,188}Pb and ^{194}Po. *Physical Review Letters*, 97(6):062501, aug 2006.

[11] J. Pakarinen et al. Evidence for oblate structure in ^{186}Pb. *Physical Review C*, 72(1):011304R, jul 2005.

[12] J. Ojala et al. Reassigning the shapes of the 0^+ states in the ^{186}Pb nucleus. *Communications Physics*, 5(1):213, aug 2022.

[13] National nuclear data center (NNDC). http://www.nndc.bnl.gov.

[14] T. Otsuka et al. Evolution of nuclear shells due to the tensor force. *Phys. Rev. Lett.*, 95(23):232502, 2005.

[15] T. Otsuka and Y. Tsunoda. The role of shell evolution in shape coexistence. *J. of Phys. G*, 43(2):024009, feb 2016.

[16] B. A. Marsh et al. Characterization of the shape-staggering effect in mercury nuclei. *Nature Physics*, 14(12):1163–1167, Dec 2018.

[17] S. Sels et al. Shape staggering of midshell mercury isotopes from in-source laser spectroscopy compared with density-functional-theory and monte carlo shell-model calculations. *Phys. Rev. C*, 99:044306, Apr 2019.

[18] J. Pakarinen et al. Collectivity in ^{196,198}Pb isotopes probed in Coulomb-excitation experiments at REX-ISOLDE. *Journal of Physics G: Nuclear and Particle Physics*, 44(6):064009, jun 2017.

[19] H. Mach et al. A method for picosecond lifetime measurements for neutron-rich nuclei. *Nucl. Instrum. Meth. A*, 280(1):49 – 72, 1989.

[20] H. Mach et al. Retardation of B(E2; $0^+ \rightarrow 2^+$) rates in $^{90-96}$Sr and strong subshell closure effects in the A$\sim$100 region. *Nucl. Phys. A*, 523:197–227, 1991.

[21] A. Dewald et al. Recoil-gated plunger lifetime measurements in ^{188}Pb. *Phys. Rev. C*, 68:034314, Sep 2003.

[22] G. D. Dracoulis et al. E3 strength of the 11^- to 8^+ isomeric decays in ^{194}Pb and ^{196}Pb and oblate deformation. *Phys. Rev. C*, 72:064319, Dec 2005.

[23] A. N. Wilson et al. On the character of three 8+ states in 192pb. *The European Physical Journal A*, 43(2):145–151, Feb 2010.

[24] M. Ionescu-Bujor et al. Shape coexistence in neutron-deficient pb nuclei probed by quadrupole moment measurements. *Physics Letters B*, 650(2):141–147, 2007.

[25] K. Van de Vel et al. Identification of low-lying proton-based intruder states in $^{189--193}$Pb. *Phys. Rev. C*, 65:064301, May 2002.

[26] J. Griffin et al. Decay of mass-separated 3.0 min 195gbi to levels in 195pb and shape coexistence in the neutron-deficient odd-mass pb isotopes. *Nuclear Physics A*, 530(2):401–419, 1991.

[27] J. Vanhorenbeeck et al. Highly converted transitions in 197pb: Evidence for shape coexistence. *Nuclear Physics A*, 531(1):63–76, 1991.

[28] T. E. Cocolios et al. Structure of 191pb from α- and β-decay spectroscopy. *Journal of Physics G: Nuclear and Particle Physics*, 37(12):125103, nov 2010.

[29] ISOLDE yield database (development version). `https://isoyields2.web.cern.ch/YieldDetail.aspx?Z=83`.

[30] The ISOLDE RILIS. http://rilis.web.cern.ch/.

Appendix

DESCRIPTION OF THE PROPOSED EXPERIMENT

Please describe here below the main parts of your experimental set-up:

Part of the experiment	Design and manufacturing
Isolde Decay Station IDS	☒ To be used without any modification ☐ To be modified

HAZARDS GENERATED BY THE EXPERIMENT

Additional hazard from flexible or transported equipment to the CERN site:

Domain	Hazards/Hazardous Activities		Description
Mechanical Safety	Pressure	☐	[pressure] [bar], [volume][l]
	Vacuum	☐	
	Machine tools	☐	
	Mechanical energy (moving parts)	☐	
	Hot/Cold surfaces	☐	
Cryogenic Safety	Cryogenic fluid	☐	[fluid] [m3]
Electrical Safety	Electrical equipment and installations	☐	[voltage] [V], [current] [A]
	High Voltage equipment	☐	[voltage] [V]
Chemical Safety	CMR (carcinogens, mutagens and toxic to reproduction)	☐	[fluid], [quantity]
	Toxic/Irritant	☐	[fluid], [quantity]
	Corrosive	☐	[fluid], [quantity]
	Oxidizing	☐	[fluid], [quantity]
	Flammable/Potentially explosive atmospheres	☐	[fluid], [quantity]
	Dangerous for the environment	☐	[fluid], [quantity]
Non-ionizing radiation Safety	Laser	☐	[laser], [class]
	UV light	☐	
	Magnetic field	☐	[magnetic field] [T]
Workplace	Excessive noise	☐	
	Working outside normal working hours	☐	
	Working at height (climbing platforms, etc.)	☐	
	Outdoor activities	☐	
Fire Safety	Ignition sources	☐	
	Combustible Materials	☐	
	Hot Work (e.g. welding, grinding)	☐	
Other hazards			